



Contents lists available at ScienceDirect

Bioorganic & Medicinal Chemistry

journal homepage: www.elsevier.com/locate/bmc

Pyrazole antagonists of the CB1 receptor with reduced brain penetration

Alan Fulp, Yanan Zhang, Katherine Bortoff, Herbert Seltzman, Rodney Snyder, Robert Wiethe, George Amato, Rangan Maitra*

Discovery Science and Technology, RTI International, 3040 Cornwallis Rd., Research Triangle Park, NC 27709-2194, USA

ARTICLE INFO

Article history:

Received 5 November 2015

Revised 6 January 2016

Accepted 17 January 2016

Available online xxxx

Keywords:

CB1

Cannabinoid

Peripheral

Antagonist

Rimonabant

Pyrazole

CB2

MDCK

PAMPA

Blood brain barrier

ABSTRACT

Type 1 cannabinoid receptor (CB1) antagonists might be useful for treating obesity, liver disease, metabolic syndrome, and dyslipidemias. Unfortunately, inhibition of CB1 in the central nervous system (CNS) produces adverse effects, including depression, anxiety and suicidal ideation in some patients, which led to withdrawal of the pyrazole inverse agonist rimonabant (SR141716A) from European markets. Efforts are underway to produce peripherally selective CB1 antagonists to circumvent CNS-associated adverse effects. In this study, novel analogs of rimonabant (**1**) were explored in which the 1-aminopiperidine group was switched to a 4-aminopiperidine, attached at the 4-amino position (**5**). The piperidine nitrogen was functionalized with carbamates, amides, and sulfonamides, providing compounds that are potent inverse agonists of hCB1 with good selectivity for hCB1 over hCB2. Select compounds were further studied using in vitro models of brain penetration, oral absorption and metabolic stability. Several compounds were identified with predicted minimal brain penetration and good metabolic stability. In vivo pharmacokinetic testing revealed that inverse agonist **8c** is orally bioavailable and has vastly reduced brain penetration compared to rimonabant.

© 2016 Published by Elsevier Ltd.

1. Introduction

The endocannabinoid (EC) system is comprised of endocannabinoids, receptors, transporters, and enzymes involved in the synthesis and degradation of endocannabinoids. Cannabinoid receptors, CB1 and CB2, are G protein-coupled receptors (GPCRs) whose primary function is to activate G proteins ($G_{i/o}$).¹ While CB1 is present throughout the body, it is primarily expressed in the central nervous system (CNS).² In contrast, CB2 is nominally expressed in the CNS, but is highly expressed in the human immune system.³

While agonism of the CB1 receptor is most well known as a target of drug abuse,⁴ CB1 antagonists have received attention as

potential medications for CNS related disorders including alcoholism and drug dependence.^{5,6} Additionally, through both peripheral and CNS mechanisms, the CB1 receptor has been validated as a target for the treatment of obesity, liver disease, metabolic syndrome, and dyslipidemias.^{7,8} Unfortunately, due to adverse CNS-related side effects, anxiety and depression, the first clinically approved CB1 antagonist/inverse agonist, rimonabant (SR141716A, **1**) (Fig. 1) was withdrawn from European markets. Furthermore, the adverse side effects seen with **1** precipitated the withdrawal of other CB1 antagonists, otenabant (**2**), taranabant, and ibipinabant, from clinical development.⁷

In hope of avoiding CNS-related side effects, an alternate strategy has been developed which selectively targets the CB1 receptors in the periphery for indications such as obesity, diabetes, and liver diseases. By developing CB1 antagonists that do not cross the blood–brain barrier (BBB), it is reasonable to assume that CNS side effects can be mitigated. A similar strategy has been previously used to develop peripherally selective opioids.⁹ This strategy is currently being pursued for the CB1 receptor system by several groups.¹⁰ One common approach to limit compounds to the periphery is to considerably increase their topological polar surface area (TPSA). Using this strategy, some pyrazole CB1 antagonists

Abbreviations: BBB, blood–brain barrier; BOP, benzotriazol-1-yl-oxytris (dimethylamino)phosphonium hexafluorophosphate; CB, cannabinoid receptors; CB1, cannabinoid receptor 1; CB2, cannabinoid receptor 2; CHO-K1, Chinese hamster ovary cells; CMA 80, 80% chloroform, 18% methanol, and 2% ammonium hydroxide; CNS, central nervous system; K_e , apparent affinity constant; MDCK-mdr1, Madin–Darby canine kidney cells transfected with the human MDR1 gene; IP₃, inositol phosphatase 3; MRM, multiple reaction monitoring; NA, not applicable; PAMPA, parallel artificial membrane permeability assay.

* Corresponding author. Tel.: +1 919 541 6795; fax: +1 919 541 8868.

E-mail address: rmaitra@rti.org (R. Maitra).

<http://dx.doi.org/10.1016/j.bmc.2016.01.033>

0968-0896/© 2016 Published by Elsevier Ltd.

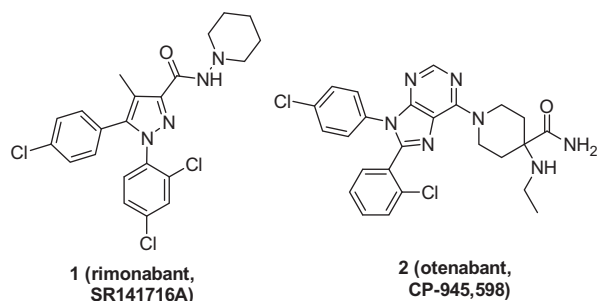


Figure 1. Examples of reported CB1 antagonists.

have been reported. These compounds include structural modifications at the 4-methyl,^{11,12} the 5-aryl position,¹³ as well as the 1-aryl position of rimonabant.¹⁴ While further characterization and validation of these compounds are required, such peripherally selective CB1 antagonists hold much promise.

Our group has been focusing on introducing changes at the 3-position of the pyrazole that increase the TPSA relative to rimonabant (Fig. 2).^{15,17} We recently reported peripherally selective CB1 antagonists based on the scaffold of rimonabant, including compounds **3** and **4** (Fig. 2).^{15–18} Both **3** and **4** were found to have brain to plasma ratios that were <0.04 when dosed at 10 mg/kg ip in Sprague-Dawley rats. When un-perfused brains are used, the cerebral blood volume present in rodent brains is 4–6%; therefore, a brain to plasma ratio of ≤ 0.04 represents little to no brain penetration.^{19–21} Unfortunately, neither **3** nor **4** are orally bioavailable. While the SAR of **3** have been extensively studied in our earlier work, the SAR requirement for **4** remained unclear.¹⁵ The molecular weight of compounds based on **4** also have the advantage of being lower compared to **3**. Our previous structural modifications mainly focused on compounds with the piperidine nitrogen functionalized as a urea. Herein we will describe our efforts to broaden the SAR around **4** to include additional carbamates, amides and sulfonamides. The *in vitro* pharmacological characterization of these compounds, including predictive assays for CNS penetration and oral absorption were conducted, leading to identification of **8c** for further testing. *In vivo* pharmacokinetic (PK) testing was performed, thus revealing that **8c** is orally bioavailable and has reduced brain penetration.

2. Results and discussion

2.1. Compound design and synthesis

The new analogs developed have been designed to broaden the SAR around **5** by examining functionalization of the piperidine

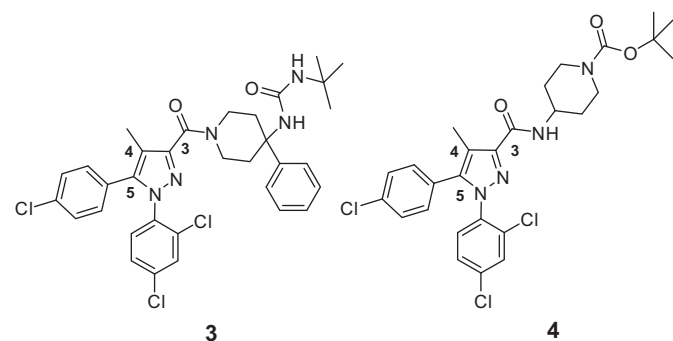


Figure 2. Peripherally selective CB1 antagonists.

nitrogen as carbamates, amides, and sulfonamides (Fig. 3). This strategy has been proven successful at discovering potent and selective analogs of both rimonabant (**1**) and otenabant (**2**).^{15–18} In the SAR studies of compound **4**, one of the goals was good oral bioavailability. A perceived advantage with compound **4** compared to **3** was its lower molecular weight, which enabled exploration of larger R groups while keeping the MW <600. The TPSA was generally kept between 60 and 90 Å² to potentially minimize CNS penetration while not precluding oral absorption.

Syntheses were carried out under standard conditions (Scheme 1). The preparation of carbamates **8a–e** began with reacting the previously reported amine **6**¹⁵ with 4-nitrophenyl chloroformate to form intermediate **7** in 75% yield. Reaction of **7** with the appropriate alcohol afforded the desired carbamate in yields ranging from 46% to 88%. Amides **9c–f** were prepared in 79–99% yield by coupling the appropriate carboxylic acid and **6** using (benzotriazol-1-yloxy)tris(dimethylamino)phosphonium hexafluorophosphate (BOP). Compound **9g** was obtained by reacting **6** with benzoyl chloride in 82% yield. Finally, **9b** was prepared in 99% yield by reacting **6** with trifluoroacetic anhydride. The synthesis of sulfonamides **10a–f** were accomplished by coupling **6** and the appropriate sulfonyl chloride in yields ranging from 57% to 85%.

2.2. Pharmacological characterization

All target compounds were pharmacologically evaluated in FLIPR-based calcium mobilization assay for hCB1 (Table 1).^{15,16} The potency of each compound was first determined in the calcium assay. Those that demonstrated apparent antagonist dissociation equilibrium constant $K_e < 50$ nM were further tested for affinity at hCB1 and selectivity for hCB1 over hCB2 using radioligand displacement of [³H]CP55940 in purified membrane fractions overexpressing either human CB1 or CB2.^{15,16} As previously reported by our group, the parent amine **6** had a $K_e > 1$ μM at the hCB1 receptor in the calcium assays.¹⁵ Most target compounds reported in this publication were found to be potent antagonists of the hCB1 receptor and several had K_e values at hCB1 of ≤ 20 nM in the calcium assays against agonist CP55940. In addition, most compounds had high affinity for the hCB1 receptor. While the aryl carbamate **7** had significantly decreased potency, the alkyl carbamates **8a–e** were all active at the hCB1 receptor in both assays. Alkyl groups smaller than the *t*-butyl in **4** were well tolerated. In particular, the ethyl, propyl and isopropyl carbamates, **8b**, **8c** and **8e**, respectively, showed good potency, affinity and selectivity. These carbamates are potentially less acid labile than **4**, which may be important for oral bioavailability. In the amide series, straight chain alkyl, branched chain alkyl, cyclic alkyl and aryl groups were active as well. The trifluoromethyl, cyclopentyl and phenyl amides (**9b**, **9f** and **9g**, respectively) were particularly potent and selective.

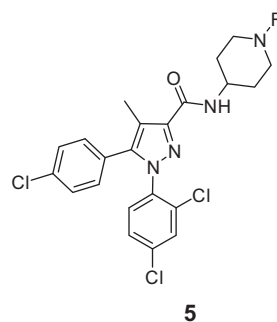
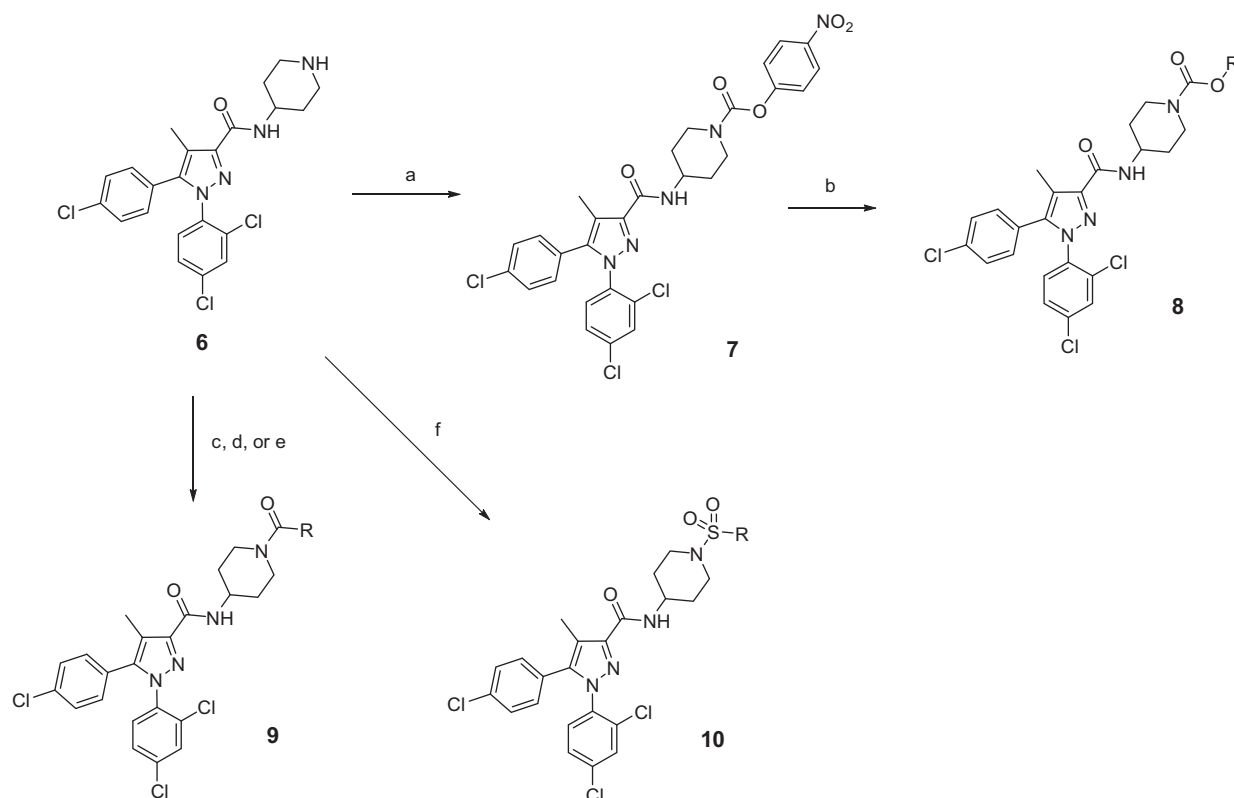


Figure 3. General strategy for SAR studies.



Scheme 1. Reagents and conditions: (a) 4-nitrophenyl chloroformate, NEt_3 , THF; (b) ROH, NaH, THF; (c) RCO_2H , BOP, NEt_3 , THF; (d) benzoyl chloride, NEt_3 , THF; (e) trifluoroacetic anhydride, NEt_3 , THF; (f) RSO_2Cl , NEt_3 , THF.

Table 1
Pharmacological characteristics of hCB1 antagonists

#	R	TPSA (\AA^2)	K_e hCB1 (nM)	K_i hCB1 ^a (nM)	K_i hCB2 ^a (nM)	Selectivity CB2/CB1
1	Rimonabant	50	1.1	6.2	313	51
6^b	Unsubstituted piperidine	59	5115			
8a	Me	76	59			
8b^b	Et	76	3	9.2	3000	326
8c	<i>n</i> -Pr	76	12	8.82	1545	175
8d	<i>n</i> -Bu	76	88			
8e	<i>i</i> -Pr	76	20	6.4	1929	301
8f^b (4)	<i>t</i> -Bu	76	4.7	2.9	2510	878
7	<i>p</i> -NO ₂ -Ph	122	212			
9a^b	Me	67	195	65	2240	34
9b	CF ₃	67	0.67	1.9	1041	548
9c	<i>n</i> -Bu	67	9.1	14.5	1785	123
9d	<i>i</i> -Bu	67	16.0	28.9	1808	63
9e		70	2198			
9f	<i>c</i> -Pen	67	3.6	9.2	2496	271
9g	Ph	67	7.0	7.5	1725	230
10a^b	Me	93	269			
10b	Et	84	18.7	44.4	4407	99
10c		84	4.3	9.6	4719	492
10d	<i>i</i> -Bu	84	9.9	43.5	6213	143
10e	<i>c</i> -Pr	84	292			
10f	Ph	84	45.8	43.0	>20000	>465

^a Displacement was measured using [³H]CP55940 in CHO cell membrane preparations overexpressing human CB1 or CB2 receptors.

^b Our previous results from Ref. 15.

The small, but electron withdrawing CF₃ group of analog **9b** provided the most potent compound of the series, demonstrating potency and affinity better than **4** and comparable to **1**. This is in stark contrast to the result for the methyl amide **9a**, which is much

less active. Compared to the potent *i*-butyl amide **9d**, the sterically similar dimethylamine analog **9e** was much less active, indicating low tolerance for a basic amine in this region. The sulfonamides showed a similar trend as the amides. Both alkyl (**10b**, **10c**, **10d**)

and aryl (**10f**) groups provided compounds with good activity. The size of the group is important, as demonstrated by the tenfold increase in potency of the ethyl sulfonamide **10b** compared to the methyl sulfonamide **10a**. Interestingly, the 3,3,3-trifluoropropyl analog (**10c**) was the most potent and selective of the sulfonamides, demonstrating similar potency and affinity as **4**.

In summary, it was shown that potent & selective compounds can be made when compound **5** is either an amide, sulfonamide or carbamate. Straight chain alkyl, branched chain alkyl, cycloalkyl and aryl groups are well tolerated. The small, but electron withdrawing trifluoromethyl amide **9f** was the most potent and selective of the compounds prepared. All compounds tested in the radioligand binding assays were highly selective with at least >50-fold selectivity for hCB1 over hCB2.

2.3. Compound **8c** is an inverse agonist of hCB1 receptor

Compound **8c** was further characterized using the calcium assay to establish whether this compound acted as a neutral antagonist or inverse agonist of hCB1 receptor. Structurally related rimonabant is an inverse agonist. As indicated by Figure 4, both compounds are inverse agonists of hCB1 as constitutive signaling through hCB1 was suppressed with increasing concentration of each compound. The EC₅₀ of **8c** was 20 nM compared to 5 nM for rimonabant.

2.4. In vitro permeability and metabolic stability testing

Select compounds were further tested in an in vitro model of BBB penetration comprising monolayers of MDCK cells expressing the human P-glycoprotein efflux transporter (MDCK-mdr1) cells grown on filters.²² Permeability of the compounds across the monolayer from the top (apical, A) to the bottom (basal, B) compartment approximates brain penetration. Caffeine is included as a reference compound that has good brain penetration. The compounds tested had little to no permeability (expressed as % transported A to B) across monolayers as indicated in Table 2. It is currently unknown whether the lack of transport noted with these

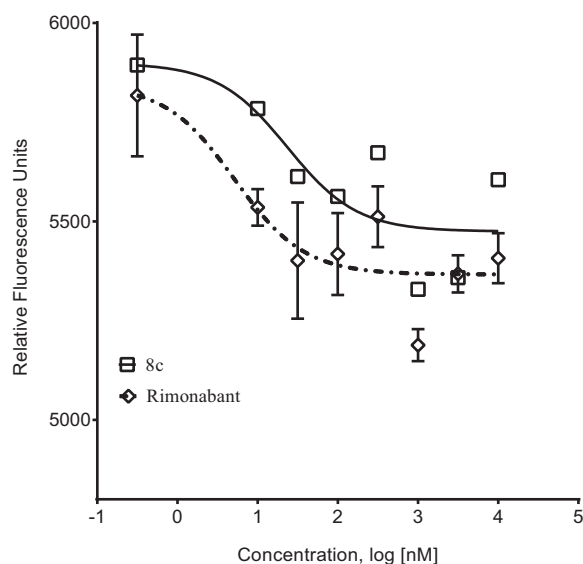
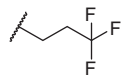


Figure 4. Compound **8c** is an inverse agonist of hCB1. CHO-CB1 cells were loaded with calcium indicator dye for 60 min as has been described in Section 4. Cells were then stimulated by various concentrations of each compound and fluorescence change recorded using FLIPR Tera (Molecular Devices) instrument. Data reported as Mean \pm SEM from 3 independent measurements.

Table 2
ADME properties of CB1 antagonists

#	R	MDCK-mdr1 A to B ^a (%)	S9% remaining at 60 min	PAMPA A to B (%) ^a pH 7.4, 5.5
8c	<i>n</i> -Pr	<1	66	1.9, 1.4
8e	<i>i</i> -Pr	<1	82	0.1, 0
9b	CF ₃	<1	74	0.2, 0.4
9c	<i>n</i> -Bu	<1	72	1.8, 1.1
9d	<i>i</i> -Bu	1	72	3.6, 3.3
9f	<i>c</i> -Pen	<1	62	0.2, 0.2
9g	Ph	<1	>90	0.2, 0.3
10b	Et	<1	68	0.05, 0.1
10c		<1	>90	0.1, 0.1
10d	<i>i</i> -Bu	<1	>90	0.2, 0.1
10f	Ph	<1	>90	0.1, 0.03
11	Caffeine	80		70, 67

^a % transported from apical (A) to basal (B) side.

compounds is related to efflux by P-glycoprotein or a function of increased TPSA.

In vitro stability of the compounds was evaluated in pooled human S9 liver fractions (Table 2). Compounds that are >50% stable after a 30 or 60 min incubation period are generally considered favorable in this assay. In general, these compounds were stable, assuaging any concerns related to poor metabolic stability. The phenyl amide **9g**, the alkyl sulfonamides **10c** and **10d**, and the phenyl sulfonamide **10f** demonstrated particularly high stability with >90% of the parent surviving the incubations.

PAMPA was used to predict oral absorption of these compounds. Testing was performed at pH 7.4 and 5.5 to mimic the varying pH in the intestines and allow for possible effects of compound ionization (Table 2).^{23,24} Efficient apical to basal transport, mimicking transcellular and paracellular transport across membranes coated with a lipid mixture, indicates possibility of good oral absorption in vivo. Caffeine was included as a reference compound with good permeability. Most compounds tested demonstrated low permeability in the PAMPA system, indicative of limited oral absorption. Similar results were obtained at both neutral and acidic pH. Three compounds, the *n*-propyl carbamate **8c** and the *n*-butyl and *i*-butyl amides **9c** and **9d**, however, showed some permeability. Compound **8c** is a close analog of the previously reported *t*-butyl carbamate **4**. In rats, **4** has a good brain to plasma ratio but is not orally bioavailable.¹⁵ It was hypothesized that the lack of oral bioavailability of **4** may be due to the potential instability of the *t*-butyl carbamate group in the acidic parts of the digestive tract. In compound **8c**, the *t*-butyl group is replaced with a more stable *n*-propyl group and hence this compound was selected for additional testing.

2.5. In vivo snapshot testing of compound **8c**

Compound **8c** was subjected to snapshot PK testing to assess whether this compound had limited brain exposure. As such, three 12 week old male Sprague Dawley rats were administered a bolus dose of **8c** by oral gavage. Animals were sacrificed 4 h after dosing. Samples were collected and concentration of the parent compound

Table 3
Rat brain & plasma levels of **8c**, 4 h after administration of 10 mg/kg po

Tissue	Mean	SD
Brain (ng/g)	69	8
Plasma (ng/ml)	455	95
Ratio (%)	15	3

was determined in plasma and brain. As demonstrated in Table 3, compound **8c** was orally bioavailable and had limited brain penetration. Approximately 15% exposure was noted in un-perfused brain. When un-perfused brains are used, cerebral blood volume present in this tissue is 4–6% by different estimates in rodents.^{19,21} Based on this observation, compound **8c** has >9-fold selectivity for plasma versus brain. Generally speaking, compounds that have a 10-fold or greater selectivity for plasma over brain are considered peripherally selective. Compound **8c**, thus, represents a starting point for further optimization.

3. Conclusions

To avoid the psychiatric side effects associated with CB1 antagonists, peripherally restricted CB1 antagonists that have limited BBB penetration have been pursued. In this study, a series of carbamates, amides and sulfonamides with higher TPSA than **1** were synthesized and evaluated in a number of pharmacological assays. Representatives of all three compound classes were found to be potent antagonists of the hCB1 receptor with good selectivity over hCB2. Straight chain alkyl, branched chain alkyl, cyclic alkyl and aryl groups were tolerated for activity. These compounds have predicted good metabolic stability and low BBB penetration, as determined by incubation with human S9 liver fractions and MDCK-MDR1 assays, respectively. In general, predicted oral absorption was low based on results from testing in the PAMPA system. Three compounds (**8c**, **9c** and **9d**), however, were significantly better than the others and **8c** was further studied for oral PK in rats. The results indicate that **8c** is orally bioavailable and mostly compartmentalized in plasma. It has vastly reduced penetration into the CNS compared to rimonabant, which has >50% brain penetration. Compound **8c**, thus, serves as a lead structure for producing potent and selective compounds with oral bioavailability and limited CNS penetration.

The results of this study establishes a way to analyze and triage compounds for good in vitro activity, good metabolic stability, low predicted CNS penetration and high predicted oral absorption. Future studies will further refine balancing physical properties such as MW, H-bond donating groups and TPSA to obtain compounds that are potent, selective, have low CNS penetration and good oral bioavailability.

4. Experimental

4.1. Chemistry general

Purity and characterization of compounds were established by a combination of HPLC, TLC, and NMR analytical techniques described below. ¹H spectra were recorded on a Bruker Avance DPX-300 (300 MHz) spectrometer and were determined in chloroform-*d* (CDCl₃, 7.26 ppm) or methanol-*d*₄ (CD₃OD, 3.31 ppm) with tetramethylsilane (TMS, 0.00 ppm) or solvent peaks as the internal reference unless otherwise noted. Chemical shifts are reported in ppm relative to the solvent signal, and coupling constant (*J*) values are reported in hertz (Hz). Thin-layer chromatography (TLC) was performed on EMD precoated silica gel 60 F254 plates, and spots were visualized with UV light or I₂ detection. Low-resolution mass spectra were obtained using a Waters Alliance HT/Micromass ZQ system (ESI). Unless stated otherwise, all test compounds were at least 95% pure as determined by HPLC on an Agilent 1100 system using an Agilent Zorbax SB-Phenyl, 2.1 × 150 mm, 5 μm column with gradient elution using the mobile phases (A) H₂O containing 0.05% CF₃COOH and (B) Methanol. A flow rate of 1.0 mL/min was used.

4.1.1. 4-Nitrophenyl-4-[5-(4-chlorophenyl)-1-(2,4-dichlorophenyl)-4-methyl-1H-pyrazole-3-amido]piperidine-1-carboxylate (**7**)

5-(4-Chlorophenyl)-1-(2,4-dichlorophenyl)-4-methyl-*N*-(piperidin-4-yl)-1H-pyrazole-3-carboxamide **6** (61 mg, 0.132 mmol, 1 equiv), *p*-nitrophenyl chloroformate (29 mg, 0.144 mmol, 1.1 equiv), and triethylamine (0.06 mL, 0.395 mmol, 3 equiv) were stirred for 16 h in THF (2 mL). The reaction was concentrated in vacuo. The crude material was purified by column chromatography 0–100% ethyl acetate/hexanes to yield 62 mg (75%) of desired product. Compound was 91% pure by HPLC analysis. ¹H NMR (300 MHz, CDCl₃) δ ppm 1.54–1.74 (m, 2H), 2.18 (br s, 2H), 2.42 (s, 3H), 3.04–3.38 (m, 2H), 4.21–4.43 (m, 3H), 6.95 (d, *J* = 7.91 Hz, 1H), 7.10 (d, *J* = 8.29 Hz, 2H), 7.30–7.41 (m, 5H), 7.47 (s, 1H), 8.29 (d, *J* = 9.04 Hz, 2H); [M+H]⁺ 628.7.

4.1.2. General procedure for the conversion of 4-nitrophenyl 4-[5-(4-chlorophenyl)-1-(2,4-dichlorophenyl)-4-methyl-1H-pyrazole-3-amido]piperidine-1-carboxylate (**7**) into other carbamates

To 4-nitrophenyl 4-[5-(4-chlorophenyl)-1-(2,4-dichlorophenyl)-4-methyl-1H-pyrazole-3-amido]piperidine-1-carboxylate (0.02 mmol, 1 equiv) and the appropriate alcohol (0.5 mL) in THF (2 mL) was added sodium hydride 60% dispersion in mineral oil (4 mg, 0.1 mmol, 5 equiv). The reaction was stirred for 16 h and quenched with acetic acid. The reaction was concentrated in vacuo. The crude material was purified by column chromatography using 0–100% ethyl acetate/hexanes to yield desired product.

4.1.3. Methyl 4-[5-(4-chlorophenyl)-1-(2,4-dichlorophenyl)-4-methyl-1H-pyrazole-3-amido]piperidine-1-carboxylate (**8a**)

Reaction proceeded in 78% yield. ¹H NMR (300 MHz, CDCl₃) δ ppm 1.37–1.52 (m, 2H), 1.96–2.11 (m, 3H), 2.37 (s, 3H), 2.97 (t, *J* = 12.15 Hz, 2H), 3.69 (s, 3H), 3.98–4.26 (m, 3H), 6.85 (d, *J* = 8.01 Hz, 1H), 7.06 (d, *J* = 8.29 Hz, 2H), 7.27–7.34 (m, 3H), 7.43 (s, 1H); [M+H]⁺ 521.7.

4.1.4. Propyl 4-[5-(4-chlorophenyl)-1-(2,4-dichlorophenyl)-4-methyl-1H-pyrazole-3-amido]piperidine-1-carboxylate (**8c**)

Reaction proceeded in 88% yield. ¹H NMR (300 MHz, CDCl₃) δ ppm 0.90–0.99 (m, 3H), 1.40–1.53 (m, 2H), 1.60–1.72 (m, 2H), 2.02 (d, *J* = 14.13 Hz, 2H), 2.37 (s, 3H), 2.96 (t, *J* = 12.15 Hz, 2H), 4.03 (t, *J* = 6.64 Hz, 2H), 4.07–4.25 (m, 3H), 6.85 (d, *J* = 8.10 Hz, 1H), 7.06 (d, *J* = 8.38 Hz, 2H), 7.27–7.34 (m, 3H), 7.43 (d, *J* = 1.51 Hz, 1H); [M+H]⁺ 549.7.

4.1.5. Butyl 4-[5-(4-chlorophenyl)-1-(2,4-dichlorophenyl)-4-methyl-1H-pyrazole-3-amido]piperidine-1-carboxylate (**8d**)

Reaction proceeded in 51% yield. ¹H NMR (300 MHz, CDCl₃) δ ppm 0.81–0.94 (m, 3H), 1.25–1.65 (m, 6H), 1.96 (d, *J* = 12.72 Hz, 2H), 2.30 (s, 3H), 2.89 (t, *J* = 12.15 Hz, 2H), 3.93–4.18 (m, 5H), 6.78 (d, *J* = 8.10 Hz, 1H), 6.99 (d, *J* = 8.38 Hz, 2H), 7.20–7.27 (m, 3H), 7.36 (d, *J* = 1.51 Hz, 1H); [M+H]⁺ 563.5.

4.1.6. Propan-2-yl 4-[5-(4-chlorophenyl)-1-(2,4-dichlorophenyl)-4-methyl-1H-pyrazole-3-amido]piperidine-1-carboxylate (**8e**)

Reaction proceeded in 46% yield. ¹H NMR (300 MHz, CDCl₃) δ ppm 1.17 (d, *J* = 6.22 Hz, 6H), 1.28–1.46 (m, 2H), 1.87–2.02 (m, 2H), 2.30 (s, 3H), 2.87 (t, *J* = 11.87 Hz, 2H), 3.93–4.17 (m, 3H), 4.84 (dt, *J* = 12.43, 6.22 Hz, 1H), 6.78 (d, *J* = 8.10 Hz, 1H), 6.99 (d, *J* = 8.38 Hz, 2H), 7.20–7.27 (m, 3H), 7.35 (s, 1H); [M+H]⁺ 549.4.

4.1.7. General procedure for making amides, using BOP, from 5-(4-chlorophenyl)-1-(2,4-dichlorophenyl)-4-methyl-N-(piperidin-4-yl)-1H-pyrazole-3-carboxamide (6)

To a solution of 5-(4-chlorophenyl)-1-(2,4-dichlorophenyl)-4-methyl-N-(piperidin-4-yl)-1H-pyrazole-3-carboxamide (6) (20 mg, 0.043 mmol, 1 equiv) in 2 mL of THF was added triethylamine (0.02 mL, 0.13 mmol, 3 equiv), BOP (19 mg, 0.043 mmol, 1 equiv), and the appropriate carboxylic acid (1 equiv). The reaction was stirred for 16 h and then concentrated in vacuo. The crude material was purified by silica gel column chromatography using 0–100% ethyl acetate/hexane to yield compound.

4.1.8. 5-(4-Chlorophenyl)-1-(2,4-dichlorophenyl)-4-methyl-N-[1-(trifluoroacetyl)piperidin-4-yl]-1H-pyrazole-3-carboxamide (9b)

To a solution of 5-(4-chlorophenyl)-1-(2,4-dichlorophenyl)-4-methyl-N-(piperidin-4-yl)-1H-pyrazole-3-carboxamide (6) (22 mg, 0.048 mmol, 1 equiv) in 2 mL of THF was added triethylamine (0.02 mL, 0.143 mmol, 3 equiv) and trifluoromethanesulfonic anhydride (0.01 mL, 0.071 mmol, 1.5 equiv). The reaction was stirred 16 h and then concentrated in vacuo. The crude material was purified by silica gel column chromatography using 0–100% ethyl acetate/hexane to yield 25 mg (99%) of desired compound. ¹H NMR (300 MHz, CDCl₃) δ ppm 1.95–2.08 (m, 2H), 2.12–2.28 (m, 2H), 2.30–2.44 (m, 3H), 2.67–2.86 (m, 2H), 3.09–3.26 (m, 1H), 4.12 (d, *J* = 14.13 Hz, 1H), 4.64–4.74 (m, 1H), 7.07 (d, *J* = 8.29 Hz, 2H), 7.20–7.37 (m, 4H), 7.40 (d, *J* = 1.70 Hz, 1H); [M+H]⁺ 559.8.

4.1.9. 5-(4-Chlorophenyl)-1-(2,4-dichlorophenyl)-4-methyl-N-(1-pentanoylpiperidin-4-yl)-1H-pyrazole-3-carboxamide (9c)

Reaction proceeded in 89% yield. ¹H NMR (300 MHz, CDCl₃) δ ppm 0.88–0.98 (m, 3H), 1.31–1.48 (m, 4H), 1.53–1.67 (m, 2H), 2.03 (d, *J* = 11.77 Hz, 1H), 2.13 (d, *J* = 12.34 Hz, 1H), 2.27–2.41 (m, 5H), 2.70–2.86 (m, 1H), 3.18 (t, *J* = 11.68 Hz, 1H), 3.87 (d, *J* = 13.56 Hz, 1H), 4.09–4.29 (m, 1H), 4.59 (d, *J* = 13.56 Hz, 1H), 6.87 (d, *J* = 8.01 Hz, 1H), 7.06 (d, *J* = 8.48 Hz, 2H), 7.23–7.35 (m, 4H), 7.43 (d, *J* = 1.60 Hz, 1H); [M+H]⁺ 547.9.

4.1.10. 5-(4-Chlorophenyl)-1-(2,4-dichlorophenyl)-4-methyl-N-[1-(3-methylbutanoyl)piperidin-4-yl]-1H-pyrazole-3-carboxamide (9d)

Reaction proceeded in 99% yield. ¹H NMR (300 MHz, CDCl₃) δ ppm 0.86–0.95 (m, 6H), 1.29–1.45 (m, 2H), 1.93–2.09 (m, 3H), 2.11–2.20 (m, 2H), 2.30 (s, 3H), 2.71 (t, *J* = 11.54 Hz, 1H), 3.11 (t, *J* = 11.77 Hz, 1H), 3.75–3.88 (m, 1H), 4.11 (dd, *J* = 7.39, 3.53 Hz, 1H), 4.54 (d, *J* = 13.28 Hz, 1H), 6.80 (d, *J* = 8.01 Hz, 1H), 6.99 (d, *J* = 8.38 Hz, 2H), 7.14–7.29 (m, 4H), 7.36 (d, *J* = 1.70 Hz, 1H); [M+H]⁺ 547.7.

4.1.11. 5-(4-Chlorophenyl)-1-(2,4-dichlorophenyl)-N-[1-[2-(dimethylamino)acetyl]piperidin-4-yl]-4-methyl-1H-pyrazole-3-carboxamide (9e)

Reaction proceeded in 93% yield. ¹H NMR (300 MHz, CDCl₃) δ ppm 1.46 (br s, 2H), 2.02–2.16 (m, 2H), 2.27 (s, 6H), 2.37 (s, 3H), 2.73–2.88 (m, 1H), 3.07 (s, 1H), 3.10–3.23 (m, 2H), 4.04–4.28 (m, 2H), 4.47–4.63 (m, 1H), 6.85 (d, *J* = 8.01 Hz, 1H), 7.06 (d, *J* = 8.38 Hz, 2H), 7.23–7.34 (m, 4H), 7.43 (d, *J* = 1.32 Hz, 1H); [M+H]⁺ 548.8.

4.1.12. 5-(4-Chlorophenyl)-N-(1-cyclopentanecarbonylpiperidin-4-yl)-1-(2,4-dichlorophenyl)-4-methyl-1H-pyrazole-3-carboxamide (9f)

Reaction proceeded in 79% yield. ¹H NMR (300 MHz, CDCl₃) δ ppm 1.37–1.87 (m, 10 H), 1.98–2.07 (m, 1H), 2.13 (d,

J = 12.53 Hz, 1H), 2.37 (s, 3H), 2.72–2.85 (m, 1H), 2.90 (t, *J* = 7.82 Hz, 1H), 3.18 (t, *J* = 11.87 Hz, 1H), 3.98 (d, *J* = 13.56 Hz, 1H), 4.12–4.28 (m, 1H), 4.60 (d, *J* = 13.28 Hz, 1H), 6.86 (d, *J* = 8.01 Hz, 1H), 7.06 (d, *J* = 8.38 Hz, 2H), 7.21–7.36 (m, 4H), 7.43 (d, *J* = 1.51 Hz, 1H); [M+H]⁺ 559.7.

4.1.13. N-(1-Benzoylpiperidin-4-yl)-5-(4-chlorophenyl)-1-(2,4-dichlorophenyl)-4-methyl-1H-pyrazole-3-carboxamide (9g)

To a solution of 5-(4-chlorophenyl)-1-(2,4-dichlorophenyl)-4-methyl-N-(piperidin-4-yl)-1H-pyrazole-3-carboxamide (6) (23 mg, 0.050 mmol, 1 equiv) in 2 mL of THF was added triethylamine (0.02 mL, 0.15 mmol, 3 equiv) and benzoyl chloride (0.01 mL, 0.075 mmol, 1.5 equiv). The reaction was stirred for 16 h and then concentrated in vacuo. The crude material was purified by silica gel column chromatography using 0–100% ethyl acetate/hexane to yield 23 mg (82%) of desired compound. ¹H NMR (300 MHz, CDCl₃) δ ppm 1.33–1.62 (m, 2H), 1.98–2.21 (m, 2H), 2.37 (s, 3H), 2.87–3.30 (m, 2H), 3.81 (d, *J* = 17.71 Hz, 1H), 4.15–4.34 (m, 1H), 4.68 (br s, 1H), 6.90 (d, *J* = 8.01 Hz, 1H), 7.06 (d, *J* = 8.29 Hz, 2H), 7.25–7.35 (m, 4H), 7.36–7.47 (m, 5H); [M+H]⁺ 567.4.

4.1.14. General procedure for making sulfonamides from 5-(4-chlorophenyl)-1-(2,4-dichlorophenyl)-4-methyl-N-(piperidin-4-yl)-1H-pyrazole-3-carboxamide (6)

To a solution of 5-(4-chlorophenyl)-1-(2,4-dichlorophenyl)-4-methyl-N-(piperidin-4-yl)-1H-pyrazole-3-carboxamide (6) (20 mg, 0.043 mmol, 1 equiv) in 2 mL of THF was added triethylamine (0.02 mL, 0.13 mmol, 3 equiv) and the appropriate sulfonyl chloride (1 equiv). The reaction was stirred for 16 h and then concentrated in vacuo. The crude material was purified by silica gel column chromatography using 0–100% ethyl acetate/hexane to yield compound.

4.1.15. 5-(4-Chlorophenyl)-1-(2,4-dichlorophenyl)-N-[1-(ethanesulfonyl)piperidin-4-yl]-4-methyl-1H-pyrazole-3-carboxamide (10b)

Reaction proceeded in 77% yield. ¹H NMR (300 MHz, CDCl₃) δ ppm 1.37 (t, *J* = 7.39 Hz, 3H), 1.54–1.71 (m, 2H), 2.01–2.18 (m, 2H), 2.36 (s, 3H), 2.97 (q, *J* = 7.69 Hz, 4H), 3.83 (d, *J* = 12.53 Hz, 2H), 4.00–4.21 (m, 1H), 6.87 (d, *J* = 8.01 Hz, 1H), 7.06 (d, *J* = 8.29 Hz, 2H), 7.23–7.36 (m, 4H), 7.44 (s, 1H); [M+H]⁺ 555.6.

4.1.16. 5-(4-Chlorophenyl)-1-(2,4-dichlorophenyl)-4-methyl-N-[1-[(3,3,3-trifluoropropane)sulfonyl]piperidin-4-yl]-1H-pyrazole-3-carboxamide (10c)

Reaction proceeded in 78% yield. ¹H NMR (300 MHz, CDCl₃) δ ppm 1.58–1.72 (m, 2H), 2.07–2.20 (m, 2H), 2.37 (s, 3H), 2.55–2.71 (m, 2H), 2.93–3.06 (m, 2H), 3.06–3.17 (m, 2H), 3.84 (d, *J* = 12.43 Hz, 2H), 4.12 (ddt, *J* = 11.07, 7.28, 3.69 Hz, 1H), 6.88 (d, *J* = 8.01 Hz, 1H), 7.06 (d, *J* = 8.48 Hz, 2H), 7.23–7.37 (m, 4H), 7.43 (d, *J* = 1.79 Hz, 1H); [M+H]⁺ 625.7.

4.1.17. 5-(4-Chlorophenyl)-1-(2,4-dichlorophenyl)-4-methyl-N-[1-[(2-methylpropane)sulfonyl]piperidin-4-yl]-1H-pyrazole-3-carboxamide (10d)

Reaction proceeded in 57% yield. ¹H NMR (300 MHz, CDCl₃) δ ppm 1.11 (d, *J* = 6.69 Hz, 6H), 1.58–1.71 (m, 2H), 2.12 (d, *J* = 10.83 Hz, 2H), 2.22–2.32 (m, 1H), 2.32–2.40 (m, 3H), 2.76 (d, *J* = 6.50 Hz, 2H), 2.83–2.99 (m, 2H), 3.82 (d, *J* = 12.53 Hz, 2H), 3.99–4.19 (m, 1H), 6.87 (d, *J* = 8.01 Hz, 1H), 7.06 (d, *J* = 8.48 Hz, 2H), 7.21–7.36 (m, 4H), 7.43 (d, *J* = 1.70 Hz, 1H); [M+H]⁺ 583.9.

4.1.18. 5-(4-Chlorophenyl)-N-[1-(cyclopropanesulfonyl)piperidin-4-yl]-1-(2,4-dichlorophenyl)-4-methyl-1H-pyrazole-3-carboxamide (10e)

Reaction proceeded in 85% yield. ^1H NMR (300 MHz, CDCl_3) δ ppm 0.95–1.05 (m, 2H), 1.13–1.23 (m, 2H), 1.60–1.73 (m, 2H), 2.13 (d, $J = 10.55$ Hz, 2H), 2.24–2.31 (m, 1H), 2.37 (s, 3H), 2.98 (t, $J = 11.02$ Hz, 2H), 3.83 (d, $J = 12.34$ Hz, 2H), 4.00–4.21 (m, 1H), 6.87 (d, $J = 8.01$ Hz, 1H), 7.06 (d, $J = 8.38$ Hz, 2H), 7.22–7.37 (m, 4H), 7.43 (d, $J = 1.51$ Hz, 1H); $[\text{M}+\text{H}]^+$ 567.4.

4.1.19. N-[1-(Benzenesulfonyl)piperidin-4-yl]-5-(4-chlorophenyl)-1-(2,4-dichlorophenyl)-4-methyl-1H-pyrazole-3-carboxamide (10f)

Reaction proceeded in 84% yield. ^1H NMR (300 MHz, CDCl_3) δ ppm 1.56–1.72 (m, 2H), 2.04–2.14 (m, 2H), 2.33 (s, 3H), 2.46 (t, $J = 11.02$ Hz, 2H), 3.72–3.99 (m, 3H), 6.81 (d, $J = 8.10$ Hz, 1H), 7.04 (d, $J = 8.38$ Hz, 2H), 7.22–7.36 (m, 4H), 7.43 (d, $J = 1.51$ Hz, 1H), 7.49–7.68 (m, 3H), 7.78 (d, $J = 7.44$ Hz, 2H); $[\text{M}+\text{H}]^+$ 605.5.

4.2. Calcium mobilization and radioligand displacement assays

Each compound was pharmacologically characterized using a functional fluorescent CB1 activated $\text{G}\alpha_{q16}$ -coupled intracellular calcium mobilization assay in CHO-K1 cells, as has been described in our previous publications and apparent affinity (K_c) values were determined.^{15–18} Briefly, CHO-K1 cells were engineered to co-express human CB1 and $\text{G}\alpha_{q16}$. Activation of CB1 by an agonist then leads to generation of inositol phosphatase 3 (IP_3) and activation of IP_3 receptors, which leads to mobilization of intracellular calcium. Calcium flux was monitored in a 96-well format using the fluorescent dye Calcein-4 AM in an automated plate reader (Flexstation, Molecular Devices). The antagonism of a test compound was measured by its ability to shift the concentration response curve of the synthetic CB1 agonist CP55940 rightwards using the equation:

$$K_e = [\text{Ligand}]/[\text{DR} - 1]$$

where DR is the EC_{50} ratio of CP55940 in the presence or absence of a test agent.

For some assays, cells were loaded with Calcein-4 AM as described below and directly stimulated with various concentrations of a test agent for 90 s. Decrease in basal fluorescence was used in these assays to calculate EC_{50} values.

Further characterization of select compounds was performed using radioligand displacement of [^3H]CP55940 and equilibrium dissociation constant (K_i) values were determined as described previously.^{15–18,25} Selectivity of these compounds at hCB1 versus hCB2 was also determined by obtaining K_i values at either receptor in membranes of CHO cells over-expressing either receptor. Data reported are average values from 3 to 6 measurements typically with ~25% standard error.

4.3. MDCK-mdr1 permeability assays

MDCK-mdr1 cells obtained from the Netherlands Cancer Institute were grown on Transwell type filters (Corning) for 4 days to confluence in DMEM/F12 media containing 10% fetal bovine serum and antibiotics as has been described previously.¹⁷ Compounds were added to the apical side at a concentration of 10 μM in a transport buffer comprising of 1X Hank's balanced salt solution, 25 mM D -glucose and buffered with HEPES to pH 7.4. Samples were incubated for 1 h at 37 $^\circ\text{C}$ and carefully collected from both the apical and basal side of the filters. Compounds selected for MDCK-mdr1 cell assays were infused on an Applied Biosystems API-4000 mass spectrometer to optimize for analysis using multi-

ple reaction monitoring (MRM). Flow injection analysis was also conducted to optimize for mass spectrometer parameters. Samples from the apical and basolateral side of the MDCK cell assay were dried under nitrogen on a Turbovap LV. The chromatography was conducted with an Agilent 1100 binary pump with a flow rate of 0.5 mL/min. Mobile phase solvents were A, 0.1% formic acid in water, and B, 0.1% formic acid in methanol. The initial solvent conditions were 10% B for 1 min, then a gradient was used by increasing to 95% B over 5 min, then returning to initial conditions. Data reported are average values from 2 to 3 measurements.

4.4. In vitro stability testing

Stability of compounds to plasma and S9 fraction was performed as previously described.¹⁵ In vitro testing for metabolic stability was conducted in mixed gender pooled hepatic S9 fraction supplied by Xenotech, LLC, Lenexa, KS. Identity of the donors was unknown.

For the hepatic S9 metabolism studies, all samples were tested at 10 μM final concentration in a 1 mL volume containing 1 mg/mL S9. Samples were incubated in a buffer containing 50 mM potassium phosphate, pH 7.4 with 3 mM MgCl_2 and a NADPH regeneration system comprising of NADP (1 mM), glucose-6-phosphate (5 mM) and glucose-6-phosphate dehydrogenase (1 unit/mL). Triplicate samples were incubated for 60 min. Reactions were terminated by addition of 3 volumes of acetonitrile and processed as described for the MDCK-mdr1 assays, but standard curves were prepared in blank matrix for each compound for quantitative assessment. Data reported are average values from 3 measurements.

4.5. Parallel artificial membrane permeability assay (PAPMA)

PAMPA was conducted using a 96-well plate based kit from BD Biosciences (RTP, NC) and manufacturer's instructions were followed closely. Briefly, all samples were tested at 10 μM final concentration by adding them to the apical (top) compartment in PBS at pH 5.5 or 7.4. Samples were incubated at room temperature for 4 h. Apical to basal transport was evaluated by sampling from the top and bottom wells of the plate and measuring concentrations of compounds in each compartment using LC-MS. Processing and methods for analytical evaluation were similar to those described for MDCK-mdr1 transport assays. Data reported are average values from 3 measurements.

4.6. Pharmacokinetic testing

Male Sprague Dawley rats were procured from Charles River Laboratories (Durham, NC) at the age of 10 weeks and allowed to acclimate to the facility. Animals were dosed with compound **8c** at a concentration of 10 mg/kg in a vehicle comprised of 90% corn oil and 10% DMSO. Four hours after dosing, the animals were sacrificed and tissue collected for analyses essentially as described in our previous publications.¹⁸ LC-MS/MS was used for quantification of parent compound in a given tissue.

Acknowledgements

The authors would like to thank Ann Gilliam for performing the binding assays, Ms. Sherry Black and Ms. Purvi Patel for help with metabolic stability studies. We express our gratitude to the NIDA drug supply program for providing radiolabeled probes and to Dr. Brian Thomas for supplying the CB1 cells. This research was funded by research Grants AA022235 and DK100414 to R.M. from NIH.

Supplementary data

Supplementary data associated with this article can be found, in the online version, at <http://dx.doi.org/10.1016/j.bmc.2016.01.033>.

References and notes

1. Pacher, P.; Batkai, S.; Kunos, G. *Pharmacol. Rev.* **2006**, *58*, 389.
2. Reggio, P. H. *Curr. Med. Chem.* **2010**.
3. Mouslech, Z.; Valla, V. *Neuro. Endocrinol. Lett.* **2009**, *30*, 153.
4. Demuth, D. G.; Molleman, A. *Life Sci.* **2006**, *78*, 549.
5. De Vries, T. J.; Schoffemeer, A. N. *Trends Pharmacol. Sci.* **2005**, *26*, 420.
6. Le Foll, B.; Goldberg, S. R. *J. Pharmacol. Exp. Ther.* **2005**, *312*, 875.
7. Pacher, P.; Kunos, G. *FEBS J.* **2013**, *280*, 1918.
8. Janero, D. R.; Makriyannis, A. *Expert Opin. Emerg. Drugs* **2009**, *14*, 43.
9. Stein, C.; Schafer, M.; Machelska, H. *Nat. Med.* **2003**, *9*, 1003.
10. Chorvat, R. *J. Bioorg. Med. Chem. Lett.* **2013**, *23*, 4751.
11. Cooper, M.; Receveur, J. M.; Bjurling, E.; Norregaard, P. K.; Nielsen, P. A.; Skold, N.; Hogberg, T. *Bioorg. Med. Chem. Lett.* **2010**, *20*, 26.
12. Receveur, J. M.; Murray, A.; Linget, J. M.; Norregaard, P. K.; Cooper, M.; Bjurling, E.; Nielsen, P. A.; Hogberg, T. *Bioorg. Med. Chem. Lett.* **2010**, *20*, 453.
13. Hung, M. S.; Chang, C. P.; Li, T. C.; Yeh, T. K.; Song, J. S.; Lin, Y.; Wu, C. H.; Kuo, P. C.; Amancha, P. K.; Wong, Y. C.; Hsiao, W. C.; Chao, Y. S.; Shia, K. S. *ChemMedChem* **2010**, *5*, 1439.
14. Sasmal, P. K.; Reddy, D. S.; Talwar, R.; Venkatesham, B.; Balasubrahmanyam, D.; Kannan, M.; Srinivas, P.; Kumar, K. S.; Devi, B. N.; Jadhav, V. P.; Khan, S. K.; Mohan, P.; Chaudhury, H.; Bhuniya, D.; Iqbal, J.; Chakrabarti, R. *Bioorg. Med. Chem. Lett.* **2011**, *21*, 562.
15. Fulp, A.; Bortoff, K.; Seltzman, H.; Zhang, Y.; Mathews, J.; Snyder, R.; Fennell, T.; Maitra, R. *J. Med. Chem.* **2012**, *55*, 2820.
16. Fulp, A.; Bortoff, K.; Zhang, Y.; Seltzman, H.; Mathews, J.; Snyder, R.; Fennell, T.; Maitra, R. *J. Med. Chem.* **2012**, *55*, 10022.
17. Fulp, A.; Bortoff, K.; Zhang, Y.; Seltzman, H.; Snyder, R.; Maitra, R. *Bioorg. Med. Chem. Lett.* **2011**, *21*, 5711.
18. Fulp, A.; Bortoff, K.; Zhang, Y.; Snyder, R.; Fennell, T.; Marusich, J. A.; Wiley, J. L.; Seltzman, H.; Maitra, R. *J. Med. Chem.* **2013**, *56*, 8066.
19. Chugh, B. P.; Lerch, J. P.; Yu, L. X.; Pienkowski, M.; Harrison, R. V.; Henkelman, R. M.; Sled, J. G. *Neuroimage* **2009**, *47*, 1312.
20. Edvinsson, L.; Nielsen, K. C.; Owman, C. *Experientia* **1973**, *29*, 432.
21. Adam, J. F.; Elleaume, H.; Le Duc, G.; Corde, S.; Charvet, A. M.; Tropres, I.; Le Bas, J. F.; Esteve, F. *J. Cereb. Blood Flow Metab.* **2003**, *23*, 499.
22. Wang, Q.; Rager, J. D.; Weinstein, K.; Kardos, P. S.; Dobson, G. L.; Li, J.; Hidalgo, I. *J. Int. J. Pharm.* **2005**, *288*, 349.
23. Mensch, J.; Jaroskova, L.; Sanderson, W.; Melis, A.; Mackie, C.; Verreck, G.; Brewster, M. E.; Augustijns, P. *Int. J. Pharm.* **2010**, *395*, 182.
24. Mensch, J.; Melis, A.; Mackie, C.; Verreck, G.; Brewster, M. E.; Augustijns, P. *Eur. J. Pharm. Biopharm.* **2010**, *74*, 495.
25. Zhang, Y.; Gilliam, A.; Maitra, R.; Damaj, M. I.; Tajuba, J. M.; Seltzman, H. H.; Thomas, B. F. *J. Med. Chem.* **2010**, *53*, 7048.